Available online at www.sciencedirect.com
SCIENCE DIRECT®
Journal of Chromatography A, 1089 (2005) 125–134
JOURNAL OF CHROMATOGRAPHY A
www.elsevier.com/locate/chroma

Effect of microwave dielectric heating on intraparticle diffusion in reversed-phase liquid chromatography

Wilmer A. Galinada [a,b], Georges Guiochon [a,b,*]

[a] *Department of Chemistry, The University of Tennessee, Knoxville, TN 37996-1600, USA*
[b] *Division of Chemical Sciences, Oak Ridge National Laboratory, Oak Ridge, TN 37831, USA*

Received 3 March 2005; received in revised form 15 June 2005; accepted 22 June 2005

Abstract

The influence of microwave (MW) irradiation on the mass transfer kinetics in reversed-phase liquid chromatography (RPLC) was studied by placing a column in a microwave oven and measuring the incremental change in the temperature of the column effluent stream at various microwave energies and mobile phase compositions. The microwave energy dissipated in the column was set between 15 and 200 W and the mobile phase composition used varied from 100 to 70, 50, and 10% methanol in water at 1.2 mL/min. At all the mobile phase compositions considered, the effluent temperature increased with increasing microwave energy. At 70% methanol, the mobile phase flow rate was set at 1.2, 2.0, and 2.8 mL/min. At 1.2 mL/min, the effluent temperatures at the lowest (15 W) and highest (200 W) microwave energy inputs were $25 \pm 1\,^{\circ}C$ and $41 \pm 1\,^{\circ}C$ for pure methanol, $25 \pm 1\,^{\circ}C$ and $48 \pm 1\,^{\circ}C$ for 70% methanol, $25 \pm 1\,^{\circ}C$ and $50 \pm 1\,^{\circ}C$ for 50% methanol, and, $25 \pm 1\,^{\circ}C$ and $52 \pm 1\,^{\circ}C$ for 10% methanol, respectively. With 70% methanol and microwave energy inputs of 15, 30, and 50 W, the effluent temperature did not change with increasing flow rate; a considerable change was observed at 100, 150, and 200 W between 1.2 and 2.0 mL/min and none between 2.0 and 2.8 mL/min. Chromatographic elution band profiles of propylbenzene were recorded under linear conditions, in 70% methanol solutions, for microwave energy inputs of 0, 15 and 30 W, at constant temperature. The intraparticle diffusion coefficient, D_e, under microwave irradiation was ca. 20% higher than without irradiation. These preliminary results suggest that microwave irradiation may have a considerable influence on intraparticle diffusion in RPLC.

Keywords: Microwave irradiation; Dielectric heating; Mobile phase composition; Intraparticle diffusion

1. Introduction

Microwave (MW) irradiation is a well-established procedure in the industrial processing of foods, polymers and other materials. It is an important tool in the preparation of samples for many analytical methods. The speed and easy control of the heating of the feed are the main factors causing chemists to apply it in the laboratory [1]. Microwave irradiation was shown to have a significant effect on reaction rates in various synthetic and catalytic reactions, particularly in organic synthesis [1–4]. This increase in reaction rates can be very high; for instance, a 1200-fold increase in reaction rate upon irradiation was reported [5]. However, the current applications of microwave irradiation as a chemical laboratory technique have been primarily focused on sample preparations and decompositions, e.g., fusion, mineralization, ashing, extraction, and other closed-vessel chemical reactions such as the synthesis of organics, organometallics, and inorganics [1]. Its possible application to the enhancement of mass transfers in chromatographic separation processes, or more generally in liquid–solid separations remains unexplored.

A few studies have been made on the application of microwave irradiation in adsorption and desorption processes of gases on zeolites [6–7]. These studies used a packed column exposed to microwave irradiation and measured the influence of the microwave power on the rate and selectivity of the physical sorption of gases onto zeolites. Microwave

* Corresponding author. Fax: +1 865 974 2667.
E-mail address: guiochon@utk.edu (G. Guiochon).

0021-9673/$ – see front matter © 2005 Elsevier B.V. All rights reserved.
doi:10.1016/j.chroma.2005.06.062

irradiation at 2.45 GHz was also shown greatly to accelerate the diffusion of ethylene oxide in polymeric materials over conventional heating at the same temperature [2,8]. These studies demonstrated that the effects of microwave irradiation differ from those of conventional heating.

Since the fundamental methods used in gas and liquid chromatography to separate chemical constituents are similar to adsorption, the application of microwave irradiation to liquid–solid separation systems seems highly desirable. Such feasibility was explored recently [9]. In this study, microwave radiation was induced by short pulses of a domestic 600 W microwave oven at 2.45 GHz, with no power programming. The study merely compared the profiles and efficiencies of the peaks obtained with and without microwave irradiation. Although microwave irradiation was shown to enhance the separation, no quantitative measurements of the effects of the mobile phase composition, the flow rate, and the microwave energy input on microwave dielectric heating were made. The influence of microwave radiations on the individual constituents involved in the separation process was not discussed in details.

Microwaves stimulate species depending on their dielectric properties. The dielectric constant indicates the ability of a material to be polarized by an electric field, e.g., a microwave field. The dielectric constants of different molecules are widely different, with values of 78.5, 32.6, and 2.3 at 25 °C for water, methanol, and propylbenzene, respectively [10]. Pure silica has a dielectric constant close to zero. It does not heat appreciably when exposed to microwave irradiation and is considered to be fully transparent to microwave radiation [6].

To the best of our knowledge, the effects of microwave irradiation on the adsorption and desorption kinetics in liquid–solid systems, particularly on intraparticle diffusion in reversed phase liquid chromatography, have never been studied. The purpose of this study is to investigate under which experimental conditions MW irradiation could be used to enhance chromatographic separations since MW irradiation has selective and complex interactions with materials. Specifically, the effect of microwave power, mobile phase composition, and mobile phase flow rate on microwave dielectric heating in RPLC column is studied.

2. Theory

2.1. Moment analysis

The use of the general rate model of chromatography provides the only rigorous approach for a detailed investigation of the influence of the experimental conditions on the rate of the mass transfer kinetics and on the band profiles in chromatography. Although there are no algebraic solutions, only numerical solutions for this model, a solution is available for the Laplace transform in the linear case. However, this solution of the system of equations of the general rate model in the Laplace domain provides equations relating the first absolute moment and the second central moment of elution bands to the characteristics of the retention equilibrium and of the mass transfer kinetics, respectively. This approach constitutes the theoretical aspect of this work.

Chromatographic band profiles were analyzed using the conventional method of moment analysis [11–15]. This method has been previously proven to be the most effective in the accurate determination of the properties of chromatographic peaks [16–17]. It has now become the most conventional method for this kind of investigations [11]. More details on moment analysis can be found elsewhere [18–22]. Information on the thermodynamics of equilibrium between the mobile and the stationary phases, and on the mass transfer kinetics between the two phases in the column are derived from the first absolute moment (μ_1) and the second central moment (μ_2') of the bands, respectively. The definitions of the first absolute moment (μ_1) and the second central moment (μ_2') of chromatographic peaks are as follows:

$$\mu_1 = \frac{\int C(t)t\,\mathrm{d}t}{\int C(t)\,\mathrm{d}t} = \frac{L}{u_0}\delta_0 \tag{1}$$

$$\mu_2' = \frac{\int C(t)(t-\mu_1)^2\,\mathrm{d}t}{\int C(t)\,\mathrm{d}t} \tag{2}$$

where $C(t)$ is the chromatographic band profile, L the length of the column, and u_0 the mobile phase velocity. The first moment and the second central moment are related to the different characteristics of the column, as follows:

$$\mu_2' = \frac{2L}{u_0}(\delta_{ax} + \delta_f + \delta_d) + (\mu_2')_{inj} + (\mu_2')_{sys} \tag{3}$$

$$\delta_{ax} = \frac{\varepsilon_e D_L \delta_0^2}{u_0^2} \tag{4}$$

$$\delta_f = (1-\varepsilon_e)\left(\frac{R_p}{3k_{ext}}\right)(\varepsilon_p + (1-\varepsilon_p)K)^2 \tag{5}$$

$$\delta_d = (1-\varepsilon_e)\left(\frac{R_p^2}{15D_e}\right)(\varepsilon_p + (1-\varepsilon_p)K)^2 \tag{6}$$

$$\delta_0 = \varepsilon_e + (1-\varepsilon_e)(\varepsilon_p + (1-\varepsilon_p)K) \tag{7}$$

where $(\mu_2')_{inj}$ and $(\mu_2')_{sys}$ denote the extra-column contributions to the second central moment, contributions arising from the injection of the probe compound into the mobile phase stream and from the extra-column void volumes of the instrument, respectively. The terms δ_{ax}, δ_d, and δ_f account for the contributions to μ_2' of axial dispersion, the external (or fluid-to-particle) mass transfer resistance, and intraparticle diffusion, respectively. Thus, μ_2' is the sum of the contributions of three independent mass transport processes that take place in the column and of the contributions of the instrument, $(\mu_2')_{inj}$ and $(\mu_2')_{sys}$ to band broadening. It is usually assumed that the contribution of the actual rate of the adsorption/desorption on the actual adsorption sites to μ_2' is

negligibly small. This assumption has been previously validated [23]. The other parameters in the above equations are: ε_e, the external (bed) porosity; k_{ext}, the external mass transfer coefficient; D_e, the effective intraparticle diffusion coefficient; and, $K = q/C$, the equilibrium constant. The concentrations in the fluid phase, C, and at the adsorbent surface, q, are referenced to the fluid volume and to the adsorbent matrix volume, respectively.

Eq. (3) shows that the contributions of the different sources of mass transfer resistances to the second moment are separate and additive. The first and the second moments are simply related to the column efficiency (i.e., the number of theoretical plates, N, of the column) and to the height equivalent to a theoretical plate (HETP), H, namely

$$N = \frac{\mu_1^2}{\mu_2'} \tag{8}$$

$$H = \frac{L}{N} = \frac{L\mu_2'}{\mu_1^2} \tag{9}$$

By combining Eqs. (1)–(3) and Eq. (9), the general expression for H is derived:

$$H = \frac{2u_0\varepsilon_e}{\delta_0^2}(\delta_{ax} + \delta_f + \delta_d) \tag{10}$$

where $u_0 = L/t_0$ is the superficial, linear velocity. Substituting Eqs. (4)–(6) into Eq. (10) gives

$$H = \frac{2\varepsilon_e D_L}{u_0} + \frac{2u_0(1-\varepsilon_e)(\varepsilon_p + (1-\varepsilon_p)K)^2}{\delta_0^2} \times \left(\frac{R_p}{3k_{ext}} + \frac{R_p^2}{15D_e}\right) \tag{11}$$

For the sake of simplification, the following auxiliary parameters, A and H_0 are introduced:

$$A = \frac{(1-\varepsilon_e)(\varepsilon_p + (1-\varepsilon_p)K)^2}{\delta_0^2} \tag{12}$$

$$H_0 = \frac{\delta_f + \delta_d}{\delta_0^2} = A\left(\frac{R_p}{3k_{ext}} + \frac{R_p^2}{15D_e}\right) \tag{13}$$

Finally, Eq. (9) is transformed into

$$H' = \frac{H}{2u_0} = \frac{L\mu_2'}{\mu_1^2 2u_0} = \frac{\varepsilon_e D_L}{u_0^2} + H_0 \tag{14}$$

Note that the parameters H_0 and H' in Eqs. (13) and (14) are not the conventional HETPs used in HPLC that are reported in length units. They are defined and expressed in time units and are equal to the conventional HETPs divided by $2u_0$. It results from Eq. (14) that the dependence of H' on the mobile phase velocity is a combination of the effects of axial dispersion and of several mass transfer resistances. According to Eq. (14), the plot of $(\mu_2' L)/(2\mu_1^2 u_0)$ versus $1/u_0^2$ should be a straight line, having a slope and an intercept equal to the values of the coefficient of axial dispersion, D_L, and to H_0, respectively. Eq. (13) can be transformed into

$$\delta_d = H_0\delta_0^2 - \delta_f \tag{15}$$

The values of δ_f and δ_0 can be calculated by Eqs. (5) and (7), respectively. Then the value of δ_d can be derived from the value of H_0. Finally, the value of the intraparticle diffusion coefficient, D_e, is derived from the following transformation of Eq. (6):

$$D_e = \frac{R_P^2}{15\delta_d}(1-\varepsilon_e)[\varepsilon_P + (1-\varepsilon_P)K]^2 \tag{16}$$

2.2. Calculation of the thermodynamic equilibrium constant

In this work, all chromatographic measurements were conducted under linear conditions, i.e., the adsorption isotherm is assumed to be linear and the sample concentration is low enough to make it so. Therefore, the solid–liquid equilibrium is characterized only by an equilibrium constant that does not vary with the solute concentration. K is calculated by the following equations or is derived from the first moment of the band (Eq. (1)).

$$k' = \frac{t_R - t_0}{t_0} \tag{17}$$

$$\beta = \frac{V_s}{V_m} = \frac{1-\varepsilon_t}{\varepsilon_t} \tag{18}$$

$$K = \frac{k'}{\beta} \tag{19}$$

where k' is the retention factor, t_R and t_0 are the retention times of the solute and of the peak of an unretained compound, respectively, β is the phase ratio, V_m and V_s are the volumes of the mobile and the stationary phases, respectively, and ε_t is the total porosity of the column (i.e., the volume fraction of the column that is occupied by the mobile phase).

2.3. Calculation of the kinetic parameters

In this work, all the mass transfer kinetic parameters and the dispersion coefficient were determined experimentally. The results obtained were then compared with the values of these parameters derived from theoretical calculations based on most frequently used correlations.

2.3.1. External mass transfer coefficient

As shown in Eq. (5), the external mass transfer coefficient (k_{ext}) must be known to apply the moment analysis. This parameter is estimated independently, using the generally accepted empirical correlation of Wilson–Geankoplis, a correlation that is valid for $0.0015 < Re < 55$ [24].

$$Sh = \left(\frac{1.09}{\varepsilon_e}\right) Sc^{1/3} Re^{1/3} \tag{20}$$

This equation relates Sherwood number, *Sh*, a function of the external mass transfer coefficient, to the Schmidt number, *Sc*, and the Reynolds number, *Re*. These three classical non-dimensional numbers are defined by the following equations [25]:

$$Sh = \frac{k_{ext} d_p}{D_m} \tag{21}$$

$$Sc = \frac{\eta}{\rho_s D_m} \tag{22}$$

$$Re = \frac{u_0 d_p \rho_s}{\eta} \tag{23}$$

Substituting Eqs. (21)–(23) into Eq. (20) gives the external mass transfer coefficient as

$$k_{ext} = \frac{1.09(u_0)^{1/3}}{\varepsilon_e} \left(\frac{D_m}{d_p} \right)^{2/3} \tag{24}$$

where D_m is the molecular diffusivity of the solute in the mobile phase, η the mobile phase viscosity, and ρ_s its density. The above equation permits the calculation of k_{ext} when the value of D_m is known. D_m is derived from the Wilke–Chang equation, a correlation most frequently used in the HPLC literature that is claimed to be accurate within 10% for small to medium-size molecules [11,18–19,26]. Its formulation is:

$$D_m = 7.4 \times 10^{-8} T \frac{(\alpha_A M_s)^{0.5}}{\eta' V_A^{0.6}} \tag{25}$$

where T is the absolute temperature of the column, M_s the molecular weight of the fluid phase, η' the viscosity of the fluid (in cP), V_A the molar volume of the solute at its normal boiling point (calculated from LeBas correlation [27–29]), and α_A the association factor of the fluid which accounts for the solute–solvent interactions [11]. This factor is 1.9 for methanol and 2.6 for water.

2.3.2. Axial dispersion coefficient

The axial dispersion coefficient, D_L, was calculated from the Gunn equation [30]:

$$\frac{\varepsilon_e D_L}{d_p u_0} = B(1 + \sigma_v^2) + \frac{\sigma_v^2}{2} + \frac{\varepsilon_e}{\tau ReSc} \tag{26}$$

with

$$B = \left\{ \frac{ReSc}{4\alpha_1^2(1-\varepsilon_e)}(1-p)^2 + \frac{(ReSc)^2}{16\alpha_1^4(1-\varepsilon_e)^2} p(1-p)^3 \times \left[\exp\left(\frac{-4\alpha_1^2(1-\varepsilon_e)}{p(1-p)ReSc} \right) - 1 \right] \right\} \tag{27}$$

where α_1 is the first root of the zero-order Bessel function, τ is the bed package tortuosity factor (assumed to be equal to 1.4) [30], and σ_v^2 is the dimensionless variance of the distribution of the ratio between the local fluid linear velocity and the average velocity over the column cross-section. In this work, this variance was assumed to be equal to zero. Finally, p is a parameter defined by [30]:

$$p = 0.17 + 0.33 \exp\left(\frac{-24}{Re} \right) \tag{28}$$

2.3.3. Solvent-related parameters

The related parameters for the use of methanol/water mixture, which are required in the calculation of the molecular diffusivity in Eq. (25), were determined from the procedure described in the literature [31–32]. The molecular weight (M_s), the association factor (α_A), and the viscosity (η') were calculated using the following equations:

$$M_S = X_{org} M_{S,org} + X_{water} M_{S,water} \tag{29}$$

$$\alpha_A = X_{org} \alpha_{A,org} + X_{water} \alpha_{A,water} \tag{30}$$

$$\eta' = \phi_{org} \eta_{org} \exp(\phi_{water} \varphi_{water}) + \phi_{water} \eta_{water} \exp(\phi_{org} \varphi_{org}) \tag{31}$$

where X and ϕ are the mole fraction and the volume fraction of the mixture components, respectively; φ_{org} and φ_{water} are empirical parameters [11]. The subscripts "org" and "water" stand for the organic component and water, respectively.

3. Experimental

3.1. Equipment

An Ethos solvent extraction labstation (Ethos E, Milestone, Shelton, CT) was used. It is not a modified kitchen microwave unit but a rugged, heavy-duty, safe professional instrument, designed for laboratory uses. It includes three pre-fabricated holes through the top of the oven to allow microwave irradiation experiments using a continuous flow reactor for an indefinite period of time. It has an original microwave feed/distribution system to the working cavity, fed by two 800 W industrial magnetrons operating at 2.45 GHz, each with its own high voltage power supply. The system power is limited by design to 1000 W to ensure a long magnetron life. The microwaves are first fed into a premixing chamber from where a pyramid-shaped rotating metal diffuser evenly distributes the microwaves into the cavity. This unique design and its microprocessor control ensure optimal microwave distribution in the cavity, thus preventing localized "hot spots". The Ethos E includes a touch-screen controller with a software for advanced method development, archiving, and retrieval. It features a real-time graphical display of the parameters such as microwave power input, temperature, time, and pressure, which can be modified before and during operations.

An HP 1100 series (Hewlett-Packard, Palo Alto, CA) was employed for all chromatographic experimental determinations. The instrument is equipped with an isocratic pump, a thermostat, a diode array UV-spectrometric detector, and

a computer data station that controls its operation. A Rheodyne manual sample injector (model 7725(i)) with a 5-μL sample loop (Rhonert Park, CA) was used for sample injections. The UV detector signal was acquired at a wavelength of 254 nm.

3.2. Mobile phase composition and chemicals

Experiments were performed with mobile phases made of pure methanol or aqueous solutions of methanol (10, 50, and 70% methanol). Methanol and water were HPLC grade solvents from Fisher Scientific (Fair Lawn, NJ). Thiourea was purchased from Sigma Chemical Co. (St. Louis, MO). Propylbenzene was purchased from Aldrich Chemical Co. (Milwaukee, WI).

3.3. Chromatographic conditions

All experiments were carried out using a $150 \times 4.6\,mm^2$ PEEK (polyetheretherketone) column, packed by the manufacturer with Luna $C_{18}(2)$ with an average particle size of 50 μm (Phenomenex, Torrance, CA). This material is made of spherical particles of porous silica, chemically bonded with octadecylsilane (carbon load, 17.5%; pore size, 100 Å; surface area, $400\,m^2/g$; calculated bonded phase coverage, $3.0\,\mu mole/m^2$). A large average particle diameter was chosen to magnify the mass transfer resistances and to allow a better precision in the measurements of small differences between these resistances that could possibly be correlated with changes in the experimental conditions and particularly in the irradiation power applied to the column. The microwave power induced into the column was varied from 15 to 200 W.

The column was placed inside the microwave oven in a hanging position, i.e., suspended in mid-air, supported by the PEEK connecting tubings at its inlet and outlet. The inlet tubing connects the manual injector to the column and the outlet tubing connects the column to the detector. A thermocouple was placed against the tubing evacuating the eluate stream, continuously to monitor and measure the temperature of the effluent leaving the column. This thermocouple (Atkins VersaTuff Plus Model 39658, type K, Tech Instrumentation, Parker, CO) has a range from −40 to 1000 °C, with an accuracy of ±0.5 °C between −40 and 257 °C. The thermocouple probe has a 178 mm × 2 mm bendable stainless steel tip and a 1 s response time.

The chromatographic peaks were obtained at a mobile phase composition of 70% methanol. Three different mobile phase flow rates, 1.2, 2.0, and 2.8 mL/min, were used to measure the first and second moments of the elution bands. To obtain accurate results, the column was equilibrated for at least 1 h prior to any measurements after either the flow rate or the power output of the magnetrons was changed. At least three replicates were recorded for each experimental run and the average value of the band moments was used in further calculations.

3.4. Microwave dielectric heating of the column

The effect of the mobile phase composition, the flow rate, and the microwave power on microwave dielectric heating of the column was studied using the following procedure. With a mobile phase flow rate fixed at 1.2 mL/min and varying mobile phase compositions at 100, 50, and 10% methanol, the corresponding column effluent temperatures for 15, 30, 50, 100, 150, and 200 W microwave energy inputs were measured. With a mobile phase composition of 70% methanol, the corresponding column effluent temperatures were obtained at 1.2, 2.0, and 2.8 mL/min flow rates for 15, 30, 50, 100, 150, and 200 W, and at 1.2 mL/min flow rate for 16–20, 25, 75, 125, and 175 W.

To compensate for the effect of dielectric heating of the column on the mass transfer kinetics, a series of isothermal experiments and rate constants determinations were carried out in the temperature range afforded by the range of power inputs used. The characteristics of the mass transfer kinetics of propylbenzene under MW irradiation were compared with those measured without irradiation at the same outlet temperature of the mobile phase. The comparison cannot be entirely valid, however, because the temperature of a column under MW irradiation varies along its length and across its diameter, so the value measured for the rate constant is an average.

3.5. Void fraction of the column and extra-column volume measurement

The total porosity, ε_t, of the column was derived from the retention volume of thiourea, which is practically unretained on the column. The external porosity, ε_e, of the column was obtained from Hong et al. [33], who had used a column with similar properties and characteristics. The internal porosity was calculated according to the conventional equation $\varepsilon_t = \varepsilon_e + (1 - \varepsilon_e)\varepsilon_p$.

The extra-column volumes from the injection valve to the column and from the column to the detector were derived from the retention volumes of the solute measured with the instrument at each flow rate, the column being replaced with a zero-volume connector. The contributions of $(\mu'_2)_{inj}$ and $(\mu'_2)_{sys}$ to the second central moment, μ'_2, of the solute were derived and subtracted from the second moments measured for the solute.

3.6. Procedures for moment analysis

In the present work, all experiments were carried out under linear conditions with dilute solutions (ca. 650–1500 ppm) of propylbenzene. The 20-μL standard sample loop of the manual injector was replaced with a 5-μL sample loop. The corresponding elution peaks were recorded and their first and second moments determined.

The first and second moments of the peak were calculated using the built-in program of the HP ChemStation. The

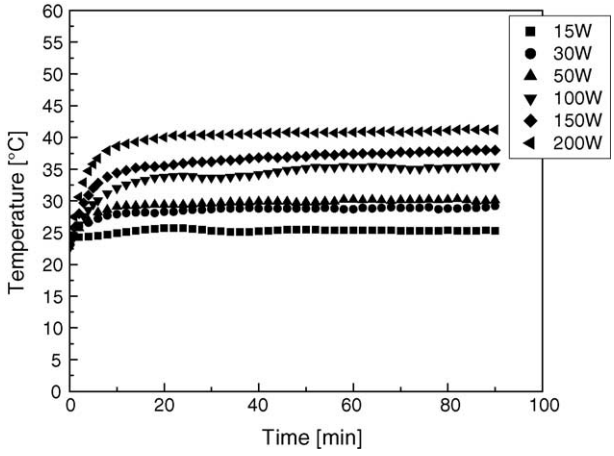

Fig. 1. Temperature profile of the mobile phase at the column outlet during the MW irradiation of the column. Mobile phase: 100–0 (pure methanol); flow rate: 1.2 mL/min; MW power input: 15–200 W.

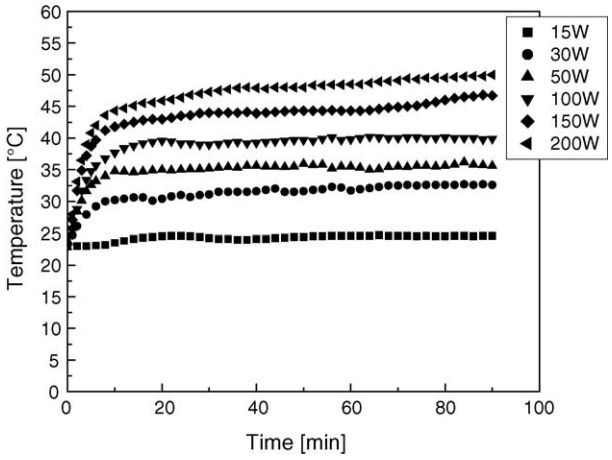

Fig. 3. Temperature profile of the mobile phase at the column outlet during the MW irradiation of the column. Mobile phase: 50–50 (methanol-water); flow rate: 1.2 mL/min; MW power input: 15–200 W.

start and end points of the peaks were automatically selected, based on the detection of the signal slope threshold. The contributions $(\mu_2')_{inj}$ and $(\mu_2')_{sys}$ were subtracted from the second central moment of the band, μ_2', to obtain the second central moment of the band and the extra-column hold-up time from the retention time of each band to obtain its first moment.

4. Results and discussion

4.1. Effect of the mobile phase composition on microwave dielectric heating

Figs. 1–4 show the temperature profiles measured at the column outlet, upon beginning MW heating, with mobile phase compositions of 100, 70, 50, and 10% methanol for 15, 30, 50, 100, 150, and 200 W microwave power input, respectively. The mobile phase flow rate was kept at 1.2 mL/min. For all mobile phase compositions considered, the MW dielectric heating increased with increasing power input. Regardless of the mobile phase composition, it was very rapid in the first few minutes and eventually stabilized after about 1 h. The corresponding effluent temperatures at the lowest (15 W) and the highest (200 W) power input were $25 \pm 1\,^{\circ}C$ and $41 \pm 1\,^{\circ}C$ for pure methanol, $25 \pm 1\,^{\circ}C$ and $48 \pm 1\,^{\circ}C$ for 70% methanol, $25 \pm 1\,^{\circ}C$ and $50 \pm 1\,^{\circ}C$ for 50% methanol, and, $25 \pm 1\,^{\circ}C$ and $52 \pm 1\,^{\circ}C$ for 10% methanol. These results show that the mobile phase composition has a considerable effect on the MW dielectric heating. Specifically, the larger the water concentration in the mobile phase, the higher the effluent temperature. This is explained by the difference between the dielectric constants of water (78.54 at $25\,^{\circ}C$) and methanol (32.63). However, the mobile phase composition has no practical effect on MW dielectric heating at the lowest (15 W) microwave power input considered.

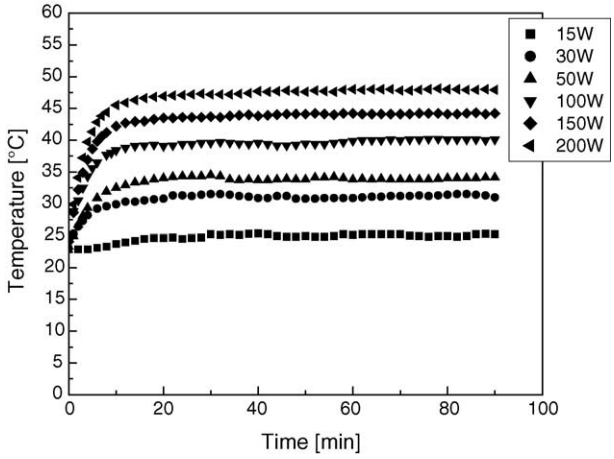

Fig. 2. Temperature profile of the mobile phase at the column outlet during the MW irradiation of the column. Mobile phase: 70–30 (methanol-water); flow rate: 1.2 mL/min; MW power input: 15–200 W.

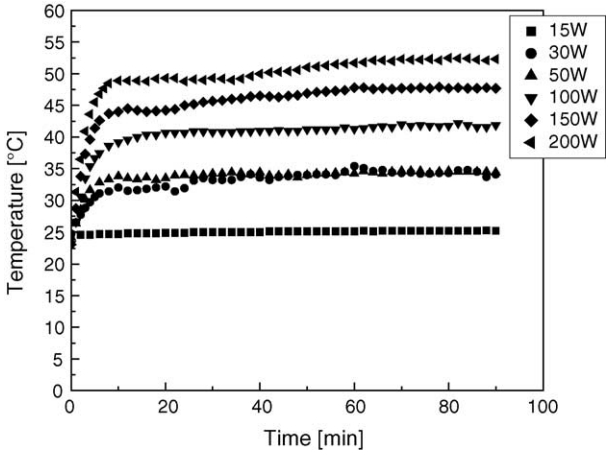

Fig. 4. Effect of mobile phase composition on microwave dielectric heating. (Mobile phase: 10–90 (methanol-water); flow rate: 1.2 mL/min; MW power input: 15–200 W).

In order to determine the maximum amount of energy that can be generated in the column without causing significant dielectric heating, measurements of the effluent temperature profile at power inputs from 16 to 25 W were made. The mobile phase composition and the flow rate were kept at 70% methanol and 1.2 mL/min, respectively. Fig. 5 shows the influence of MW heating on the temperature of the column effluent stream. This temperature remains constant at $25 \pm 1\,^{\circ}C$ for powers below 20 W and gradually increases to $27 \pm 1\,^{\circ}C$ between 20 and 25 W.

4.2. Effect of the mobile phase flow rate on microwave dielectric heating

The effect of the mobile phase flow rate on MW heating was measured at flow rates of 1.2, 2.0, and 2.8 mL/min of a 70% methanol solution. The power inputs were 15, 16–20, 30, 50, 100, 150, and 200 W. Fig. 6 shows the temperature profiles of the column effluent at 15, 50, 100, and 200 W. The profiles for 16–20 W were shown in Fig. 5. It seems that the mobile phase flow rate has no or very little effect on the temperature for 15–50 W inputs but a considerable effect at 100–200 W. However, this effect is significant mostly when the mobile phase flow rate is increased from 1.2 to 2.0 mL/min and is negligible when the flow rate is increased from 2.0 to 2.8 mL/min.

4.3. Effect of the microwave power input on microwave dielectric heating

The temperature profiles of the column effluent for power inputs of 15, 30, 50, 100, 150, and 200 W with mobile phase compositions of 100, 70, 50, and 10% methanol are shown in Figs. 1–4, respectively. The mobile phase flow rate was fixed at 1.2 mL/min. Also, MW dielectric heating increased with increasing power input for all mobile phase compositions considered. Fig. 7 shows the temperature profiles of the column eluent at the lowest (15 W) and highest (200 W) microwave power input for all mobile phase compositions. A 15 W energy input has no effect on MW dielectric heating for all mobile phase compositions studied. In contrast, at 200 W, the power input has a strong effect on the temperature profiles and this effect increases with increasing water content of the mobile phase.

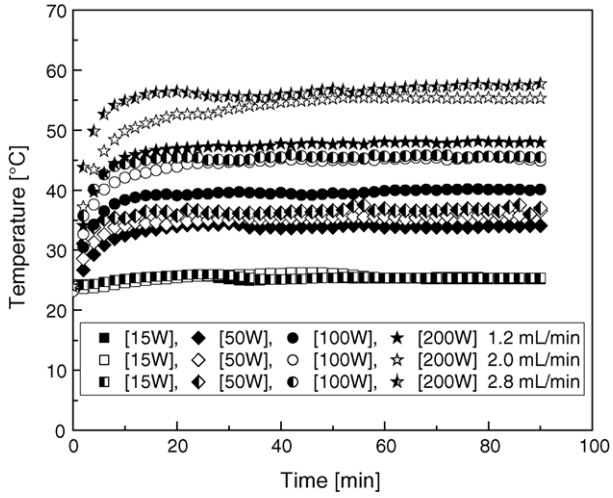

Fig. 6. Effect of the mobile phase flow rate on MW dielectric heating. Flow rate: 1.2, 2.0 and 2.8 mL/min; mobile phase: 70–30 (methanol-water); MW power input: 15, 50, 100, and 200 W.

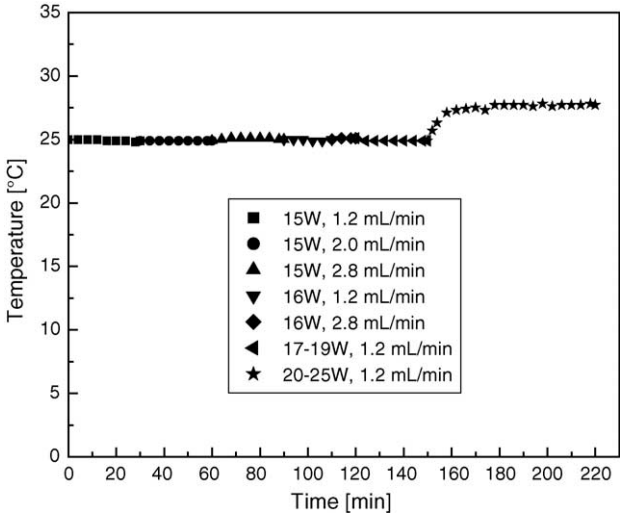

Fig. 5. Effect of the mobile phase flow rate on MW dielectric heating. Flow rate: 1.2, 2.0 and 2.8 mL/min; mobile phase: 70–30 (methanol-water); MW power input: 15 W.

4.4. Effect of microwave irradiation on intraparticle diffusion in RPLC

The effect of microwave irradiation at 15 and 30 W power input on intraparticle diffusion in RPLC was studied. Samples

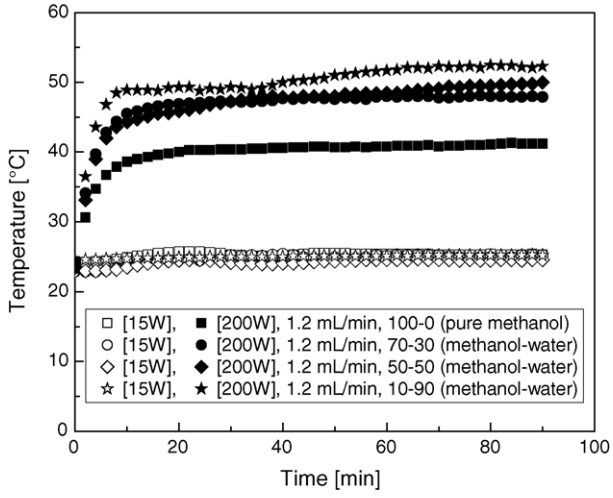

Fig. 7. Effect of the MW power input on the MW dielectric heating. Flow rate: 1.2 mL/min; mobile phase: 100–0, 70–30, 50–50, 10–90 (methanol-water); MW power input: 15 and 200 W.

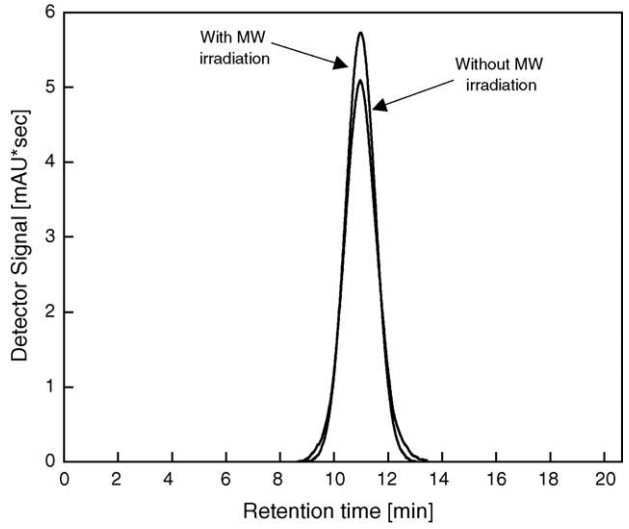

Fig. 8. Typical example of an experimental chromatogram of propylbenzene obtained with and without MW irradiation. Concentration: 1.316 g/L; injection volume: 5 μL; MW input power: 30 W; mobile phase: 70–30 (methanol-water); flow rate: 1.2 mL/min.

of propylbenzene solutions at various concentrations were injected into the column under the chromatographic conditions described earlier (Section 2).

Fig. 8 compares typical chromatograms obtained with and without MW irradiation but under otherwise identical conditions. The peak was recorded with a 70% methanol mobile phase composition, at a 1.2 mL/min flow rate and with a 30 W MW power input. The effluent temperature at this particular power input was $30 \pm 1\,^{\circ}C$. The band profile obtained with MW irradiation is sharper than without irradiation. This sharpening of the peak is due to an increase in the intraparticle diffusivity of the solute inside the particle pores, as explained later and as was illustrated in an earlier publication [9]. However, the effect was more pronounced in that earlier study due to the use of a higher power input, which corresponded to a steady outlet temperature of 75 °C. In this work, measurements were made using a lesser MW power input, causing a much lower increase of the effluent temperature. Thus, it can be predicted that increasing the MW power input will further increase the fluid-phase diffusivity, and that far sharper peaks could be obtained.

The first and second moments of the chromatographic band profiles acquired at different flow rates were analyzed using the following procedure. The plot of $H' = (\mu_2' L)/(2\mu_1^2 u_0)$ against $1/u_0^2$ (Eq. (14)) is a straight line with a slope and an intercept equal to the axial dispersion coefficient, D_L, and to H_0, respectively. The values of the D_L obtained increased with increasing MW power of irradiation. At 15 W microwave power input with a corresponding effluent temperature of $25 \pm 1\,^{\circ}C$, a slight increase of 4% was observed in the axial dispersion coefficient while at 30 W ($30 \pm 1\,^{\circ}C$), an increase of about 50% was observed, compared to the value obtained without irradiation (0 W–$30 \pm 1\,^{\circ}C$). The theoretical values of D_L were derived from the Gunn correlation, Eqs. (26)–(27), and compared to the experimental values. The difference between the experimental and the calculated values of D_L increases with increasing mobile phase velocity. At the lowest mobile phase velocity, the calculated dispersion coefficients are about 1.5–3 times larger than the experimental ones while at the largest mobile phase velocity used, the calculated values are about 4–8 times larger than the experimental values. This suggests that the Gunn correlation gives a good approximation of the axial dispersion coefficient only at low mobile phase velocities.

Table 1
Intraparticle diffusion coefficients of propylbenzene determined by the moment analysis method under different chromatographic conditions

Condition	D_{eff} [cm^2/sec]
0 W ($25 \pm 1\,^{\circ}C$)	6.947E-06
15 W ($25 \pm 1\,^{\circ}C$)	8.408E-06
0 W ($30 \pm 1\,^{\circ}C$)	7.848E-06
30 W ($30 \pm 1\,^{\circ}C$)	9.389E-06

Eq. (13) shows that the value of H_0 determined as the intercept of the plot of H' and $1/u_0^2$ is directly related to the rate constant of the external mass transfer, k_{ext}, and to the intraparticle effective diffusivity, D_e. Hence, the value of D_e can be obtained knowing k_{ext}. In this work, however, k_{ext} could not be obtained experimentally. It was calculated from Eq. (20) and the value of the intraparticle diffusion coefficient, D_e, was calculated according to Eqs. (4)–(7). The values obtained for D_e are summarized in Table 1.

Based on the data in Table 1, the values of D_e obtained under microwave irradiation are significantly higher than those obtained under conventional conditions at the same temperature. This result is consistent with the fact that MW irradiation has been shown to enhance the rate of diffusion of molecules which have dielectric properties rendering them sensitive to microwaves. However, the dielectric constant of propylbenzene is much smaller than those of methanol and water. According to a previous analysis of the surface diffusion of various alkylbenzenes in RPLC [34], the organic modifier is preferentially adsorbed onto the hydrophobic surface of the stationary phase. Its concentration is higher near the surface of the stationary phase or in the bonded layer than in the bulk mobile phase. Therefore, it is probable that the organic modifier, which is more strongly affected by MW irradiation because its dielectric constant is higher than that of the studied solute, contributed to the overall diffusion of the solute in the intraparticle space. Hence, D_e increased under microwave irradiation. However, the mode of action of the microwaves on the diffusion of the solute molecules inside the packing material is unclear at this time. This phenomenon is currently under investigation.

5. Conclusion

Microwave dielectric heating was shown to enhance the reaction rates of various chemical processes, including

molecular diffusivities and dispersion effects. Microwave radiations have selective and complex interactions with different materials. To understand the extent of the influence of MW irradiation on diffusion, it is necessary to separate from the experimental results the trivial underlying influence of the temperature of the solution that increases during the experiments. For this reason, we compared values of the intraparticle diffusion measured at the same effluent temperature, under MW irradiation or without it. We also had to assess the influence on the effluent temperature of the MW power input, the mobile phase composition (methanol and water) and the flow rate.

Chromatographic experiments made with and without MW irradiation in an aqueous solution of methanol (70% methanol), at three different mobile phase flow rates, and at different MW power input showed that the intraparticle diffusion of propylbenzene is markedly higher with than without MW irradiation and that it increases with increasing MW power input. This increase of the intraparticle diffusion of propylbenzene is probably mediated through a similar effect on water and methanol molecules.

Further investigations of the influence of microwave irradiation on the mass transfer kinetics in HPLC are in progress.

List of symbols

A	parameter defined by Eq. (12)
B	parameter defined by Eq. (27)
C	concentration of the solute in the bulk mobile phase
d_p	average particle diameter
D_e	intraparticle (or effective) diffusion coefficient
D_L	axial dispersion coefficient
D_m	molecular diffusion coefficient
H	height equivalent to a theoretical plate or parameter defined by Eq. (9)
H_0	parameter defined by Eq. (13)
k_{ext}	external mass transfer coefficient
k'	retention factor
K	adsorption equilibrium constant
L	column length
M_s	molecular mass
p	parameter in the Gunn equation, defined by Eq. (28)
q	concentration of the solute in the stationary phase
Re	Reynolds number ($u_0 d_p \rho_S/\eta$)
R_p	equivalent particle radius
Sc	Schmidt number ($\eta/\rho_S D_m$)
Sh	Sherwood number ($k_{ext} d_p/D_m$)
t_0	retention time of the unretained compound; void time of the column
t_R	retention time of the solute
T	absolute temperature
u_0	superficial linear velocity
V_A	molar volume of the liquid solute at its normal boiling point
V_m	volume of the mobile phase
V_S	volume of the stationary phase
X	mole fraction in the binary mixture

Greek symbols

α_A	solute–solvent interaction constant or association factor of the fluid
β	phase ratio
δ_{ax}	parameter defined by Eq. (4)
δ_d	parameter defined by Eq. (6)
δ_f	parameter defined by Eq. (5)
δ_0	parameter defined by Eq. (7)
ε_e	external porosity
ε_p	internal (particle) porosity
ε_t	total porosity
η	viscosity of the fluid phase
μ_1	first absolute moment
μ'_2	second central moment
$(\mu'_2)_{inj}$	second central moment denoted by injection volume
$(\mu'_2)_{sys}$	second central moment denoted by instrument void
ρ_p	particle density
ρ_s	fluid density
σ_v^2	dimensionless variance of the distribution of the ratio between the local fluid linear velocity and the average velocity over the column cross-section
τ	bed package tortuosity factor
ϕ	volume fraction of the binary mixture

Acknowledgements

This work was supported in part by Grant CHE-02-44693 of the National Science Foundation and by the cooperative agreement between the University of Tennessee and the Oak Ridge National Laboratory. We thank George Kabalka of the University of Tennessee for the generous loan of the Ethos E labstation and for fruitful discussions.

References

[1] H.M. Kingston, S.J. Haswell. Microwave-Enhanced Chemistry: Fundamentals, Sample Preparation, and Applications, Washington, DC, 1997.
[2] P. Lidstrom, J. Tierney, B. Wathey, J. Westman, Tetrahedron 57 (2001) 9225.
[3] A.G. Whittaker, D.M.P. Mingos, J. Microw. Power Electromagn. Energy 29 (1994) 195.
[4] S. Gabriel, E.H. Gabriel, E.H. Grant, B.S.J. Halstead, D.M.P. Mingos, Chem. Soc. Rev. 27 (1998) 213.
[5] R.N. Gedye, F.E. Smith, K.C. Wasteway, Can. J. Chem. 66 (1988) 17.
[6] M.D. Turner, R.L. Laurence, W.C. Conner, K.S. Yngvesson, AIChE J. 46 (2000) 758.
[7] S. Kobayashi, Y. Kim, C. Kenmizaki, S. Kushiyama, K. Mizuno, Chem. Lett. (1996) 769.
[8] I.P. Matthews, C. Gibson, A.H. Samuel, J. Biomed. Mater. Res. 23 (1989) 143.
[9] M.A. Stone, L.T. Taylor, J. Chromatogr. Sci. 41 (2003) 187.
[10] R.C. Weast, M.J. Astle, W.H. Beyer, CRC Handbook of Chemistry and Physics, CRC Press Inc., Boca Raton, Florida, 1987–1988.
[11] G. Guiochon, S. Golshan-Shirazi, A.M. Katti, Fundamentals of Preparative and Nonlinear Chromatography, Academic Press, Boston, MA, 1994.

[12] K. Miyabe, G. Guiochon, J. Separ. Sci. 26 (2003) 155.
[13] K. Miyabe, G. Guiochon, Adv. Chromatogr. 40 (2000) 1.
[14] K. Miyabe, G. Guiochon, Anal. Chem. 71 (1999) 889.
[15] K. Miyabe, G. Guiochon, J. Phys. Chem. B 103 (1999) 11086.
[16] E. Grushka, M.N. Myers, P.D. Schettler, J.C. Giddings, Anal. Chem. 41 (1969) 889.
[17] E. Grushka, J. Phys. Chem. 76 (1972) 2586.
[18] D.M. Ruthven, Principles of Adsorption and Adsorption Processes, John Wiley & Sons, New York, 1984.
[19] M. Suzuki, Adsorption Engineering, Kondansha/Elsevier, Tokyo/Amsterdam, 1990.
[20] E. Kucera, J. Chromatogr. 19 (1965) 237.
[21] M. Kubin, Collect. Czech Chem. Commun. 30 (1965) 2900.
[22] P. Schneider, M.J. Smith, AIChE J. 14 (1968) 762.
[23] K. Miyabe, G. Guiochon, Anal. Chem. 72 (2000) 5162.
[24] E.J. Wilson, C.J. Geankoplis, Ind. Eng. Chem. Fundam. 5 (1966) 9.
[25] R.C. Reid, J.M. Prausnitz, T.K. Sherwood, The Properties of Gases and Liquids, McGraw-Hill, New York, 1977.
[26] J.C. Giddings, Dynamics of Chromatography, Part 1: Principles and Theory, Marcel Dekker, New York, 1965.
[27] W. Schotte, Chem. Eng. J. 48 (1992) 167.
[28] S. Vafai, B.D. Drake, R.L. Smith Jr., J. Chem. Eng. Dat. 38 (1993) 125.
[29] A.L. Hines, R.N. Maddox, Mass Transfer Fundamentals and Application, Prentice-Hall, New Jersey, 1985.
[30] D. Gunn, Chem. Eng. Sci. 42 (1987) 363.
[31] J.W. Li, P.W. Carr, Anal. Chem. 69 (1997) 2530.
[32] H. Colin, J.C. Diez-Masa, G. Guiochon, J. Chromatogr. 167 (1978) 41.
[33] L. Hong, K. Kaczmarski, F. Gritti, G. Guiochon, AIChE J., in press.
[34] K. Miyabe, G. Guiochon, Anal. Chem. 73 (2001) 3096.